An Efficient Two-Photon-Generated Photoacid Applied to Positive-Tone 3D Microfabrication

Wenhui Zhou, *et al.*

Science **296**, 1106 (2002);
DOI: 10.1126/science.296.5570.1106

chanical energy conversion at a molecular level can be estimated as $\eta \approx 0.1$ from the left trace in Fig. 2, if it is assumed that each switching of a single azobenzene unit is initiated by a single photon carrying an energy of $E_{exc} = 5.5 \times 10^{-19}$ J ($\lambda = 365$ nm) (*47*).

In any case, an increased conversion efficiency will promote the application of future mechano-optical devices in high-density configurations, and the use of such molecular hybrids in more complex settings will be stimulated by improvements in their stability and their ability to interact with other components.

References and Notes

1. V. Balzani, A. Credi, F. M. Raymo, J. F. Stoddart, *Angew. Chem. Int. Ed.* **39**, 3348 (2000).
2. B. L. Feringa, R. A. van Delden, N. Koumura, E. M. Geertsema, *Chem. Rev.* **100**, 1789 (2000).
3. J. P. Collin, P. Gaviña, V. Heitz, J. P. Sauvage, *Eur. J. Inorg. Chem.* **1998**, 1 (1998).
4. J. M. Lehn, *Supramolecular Chemistry: Concepts and Perspectives* (Wiley-VCH, Weinheim, Germany, 1995).
5. G. U. Lee, D. A. Kidwell, R. J. Colton, *Langmuir* **10**, 354 (1994).
6. V. T. Moy, E.-L. Florin, H. E. Gaub, *Colloids Surf.* **93**, 343 (1994).
7. S. S. Wong, E. Joselevich, A. T. Woolley, C. L. Cheung, C. M. Lieber, *Nature* **394**, 52 (1998).
8. M. Rief, F. Oesterhelt, B. Heymann, H. E. Gaub, *Science* **275**, 1295 (1997).
9. M. Rief, M. Gautel, F. Oesterhelt, J. M. Fernandez, H. E. Gaub, *Science* **276**, 1109 (1997).
10. A. Janshoff, M. Neitzert, Y. Oberdörfer, H. Fuchs, *Angew. Chem. Int. Ed.* **39**, 3212 (2000).
11. H. Clausen-Schaumann, M. Seitz, R. Krautbauer, H. Gaub, *Curr. Opin. Chem. Biol.* **4**, 524 (2000).
12. T. Hugel, M. Seitz, *Macromol. Rapid Commun.* **22**, 989 (2001).
13. B. L. Smith *et al.*, *Nature* **399**, 761 (1999).
14. A. F. Oberhauser, P. E. Marszalek, H. P. Erickson, J. M. Fernandez, *Nature* **393**, 181 (1998).
15. F. Oesterhelt *et al.*, *Science* **288**, 143 (2000).
16. G. Binnig, C. F. Quate, C. Gerber, *Phys. Rev. Lett.* **56**, 930 (1986).
17. H. Clausen-Schaumann, M. Grandbois, H. E. Gaub, *Adv. Mater.* **10**, 949 (1998).
18. G. S. Hartley, *Nature* **140**, 281 (1937).
19. H. Rau, in *Photochromism: Molecules and Systems*, H. Dürr, H. Bouas-Laurent, Eds. (Elsevier, Amsterdam, 1990), chap. 4.
20. S. Shinkai, O. Manabe, *Top. Curr. Chem.* **121**, 76 (1984).
21. I. Willner, *Acc. Chem. Res.* **30**, 347 (1997).
22. L. Ulysse, J. Cubillos, J. Chmielewski, *J. Am. Chem. Soc.* **117**, 8466 (1995).
23. H. Asanuma, T. Ito, T. Yoshida, X. Liang, M. Komiyama, *Angew. Chem. Int. Ed.* **38**, 2393 (1999).
24. B. L. Feringa, W. F. Jager, B. de Lange, *Tetrahedron* **49**, 8267 (1993).
25. N. Tamai, H. Miyasaka, *Chem. Rev.* **100**, 1875 (2000).
26. G. S. Kumar, D. C. Neckers, *Chem. Rev.* **89**, 1915 (1989).
27. M. Irie, *Adv. Polym. Sci.* **94**, 27 (1990).
28. F. Vögtle, *Supramolecular Chemistry* (Wiley, New York, 1991).
29. F. Würthner, J. Rebek Jr., *J. Chem. Soc. Perkin Trans. 2* **1995**, 1727 (1995).
30. A. Archut, G. C. Azzellini, V. Balzani, L. De Cola, F. Vögtle, *J. Am. Chem. Soc.* **120**, 12187 (1998).
31. C. D. Eisenbach, *Polymer* **21**, 1175 (1980).
32. H. S. Blair, H. I. Pogue, E. Riordan, *Polymer* **21**, 1195 (1980).
33. L. A. Strzegowski, M. B. Martinez, D. C. Gowda, D. W. Urry, D. A. Tirrell, *J. Am. Chem. Soc.* **116**, 813 (1994).
34. F. Lagugné Labarthet *et al.*, *Phys. Chem. Chem. Phys.* **2**, 5154 (2000).
35. S. Monti, G. Orlandi, P. Palmieri, *Chem. Phys.* **71**, 87 (1982).
36. H. Rau, *J. Photochem.* **26**, 221 (1984).
37. T. Nägele, R. Hoche, W. Zinth, J. Wachtveitl, *Chem. Phys. Lett.* **272**, 489 (1997).
38. C. Renner, J. Cramer, R. Behrendt, L. Moroder, *Biopolymers* **54**, 501 (2000).
39. R. Behrendt *et al.*, *Angew. Chem. Intl. Ed.* **38**, 2771 (1999).
40. Molecular synthesis and spectroscopic details of the azobenzene polypeptides, as well as further information on the optomechanical AFM experiments, can be found on *Science* Online at www.sciencemag.org/cgi/content/full/296/5570/1103/DC1.
41. J. Fritz *et al.*, *Science* **288**, 316 (2000).
42. D. Axelrod, T. P. Burghardt, N. L. Thompson, *Annu. Rev. Biophys. Bioeng.* **13**, 247 (1984).
43. Because of the spectral overlap of the excitations of cis and trans configurations, the configuration average cannot be shifted entirely upon optical pumping. The respective resulting maximum populations are ~80% in the trans and 75% in the cis state (*38*).
44. M. Irie, Y. Hirano, S. Hashimoto, K. Hayashi, *Macromolecules* **14**, 262 (1981).
45. H. Finkelmann, E. Nishikawa, G. G. Pereira, M. Warner, *Phys. Rev. Lett.* **87**, 015501 (2001).
46. The maximum change of the azobenzene end-end distance by $\Delta d^{4-4'} \approx 0.25$ nm would then not be fully accounted for in the shortening of the polymer along the stretching direction. The assumption that full optical excitation of the polymer results in maximum trans-cis switching yields an average shortening by $\Delta l = 0.11$ nm per tripeptide monomer unit along the *z* axis.
47. Next to losses by dissipation of optical excitation energy, the spectral overlap causing incomplete trans-cis switching and the quantum yield of its electronical excitation are the intrinsic limiting factors of the azobenzene system.
48. J. M. Robertson, *J. Chem. Soc.* **1939**, 232 (1939).
49. Ab initio calculations (*35*) gave an angle of $\phi_{NNC} \approx -54°$ (Fig. 1A) for the cis configuration and $\phi_{NNC} \approx 66°$ for the trans configuration. This corresponds to x-ray and nuclear magnetic resonance experiments that gave values for the cis configuration of –55° and –50°, respectively (*38*, *48*).
50. Force extension traces were obtained from the deflection piezopath signal as described elsewhere (*12*). Indentation traces were taken before and after each set of traces to determine the exact position of the surface and therefore to allow correction for drift in the deflection and piezo signal.

51. Helpful discussions with J. Brauman, H. Grubmüller, D. Oesterhelt, C. Renner, and W. Zinth as well as technical support from AsylumResearch are gratefully acknowledged. Supported by the Deutsche Forschungsgemeinschaft, the Humboldt Foundation, and the Fonds der Chemischen Industrie.

15 January 2002; accepted 25 March 2002

An Efficient Two-Photon–Generated Photoacid Applied to Positive-Tone 3D Microfabrication

Wenhui Zhou,[1] Stephen M. Kuebler,[1] Kevin L. Braun,[1] Tianyue Yu,[3] J. Kevin Cammack,[1] Christopher K. Ober,[3]* Joseph W. Perry,[1,2]* Seth R. Marder[1,2]*

A two-photon–activatable photoacid generator, based on a *bis*[(diarylamino) styryl]benzene core with covalently attached sulfonium moieties, has been synthesized. The photoacid generator has both a large two-photon absorption cross section ($\delta = 690 \times 10^{-50}$ centimeter^4 second per photon) and a high quantum yield for the photochemical generation of acid ($\phi_H^+ = 0.5$). Under near-infrared laser irradiation, the molecule produces acid after two-photon excitation and initiates the polymerization of epoxides at an incident intensity that is one to two orders of magnitude lower than that needed for conventional ultraviolet-sensitive initiators. This photoacid generator was used in conjunction with a positive-tone chemically amplified resist for the fabrication of a three-dimensional (3D) microchannel structure.

The process of two-photon absorption (TPA) is currently being examined for a variety of applications, including three-dimensional (3D) microfabrication (*1*–*4*), ultra-high-density optical data storage (*5*), biological imaging (*6*), and the controlled release of biologically relevant species (*7*). Conventional ultraviolet (UV)–sensitive photoacid generators (PAGs), such as diaryliodonium and triarylsulfonium cations, have been used for two-photon microfabrication (*8*). However, the TPA cross sections, δ, of these initiators are typically very small ($\delta \leq 10 \times 10^{-50}$ cm^4 s per photon), and as a result they exhibit low two-photon sensitivity. Resins containing these initiators can be patterned only by means of long exposure times and high excitation intensities that frequently result in damage to the structure. Higher reliability and faster write speeds would be facilitated by molecules offering a large product of δ and the photochemical quantum yield ϕ_H^+. The design of highly photosensitive two-photon initiators requires (i) a chromophoric group with a large δ, such as two electron donors bridged by a π-conjugated system (a D-π-D structure) (*9*, *10*); (ii) a functionality that can generate the initiating species with high efficiency, such as those in UV initiators; and (iii) a mechanism through which excitation of the chromophore leads to activation of the chemical functionality, such as an electron transfer process (*2*). Here we describe the development of a high-sensitiv-

ity two-photon PAG and the application of it in 3D microfabrication by using a chemically amplified positive-tone resist.

We targeted PAGs because they can be used to activate a wide variety of reactions, including the ring opening of epoxides and oxetanes and cleavage reactions commonly used in chemically amplified positive resists (*11*, *12*). These resists can be particularly useful for high-fidelity 3D microfabrication because, relative to acrylate-based resins, they exhibit much lower shrinkage in both the exposure and development processes (*13*). Most large-δ molecules have excited states of relatively low energy because of their extended conjugation. Thus, molecules of this class typically have insufficient excited-state energy to activate direct bond cleavage after photoexcitation. We focused on the use of photoinduced electron transfer from TPA dyes to covalently linked sulfonium groups (*14*, *15*). From the electrochemical and spectroscopic measurements of Saeva (*16*, *17*) and our own studies (*9*, *10*), we determined that two-photon–excited *bis*(diphenylamino)-substituted *bis*(styryl)benzene dyes (with $\delta \sim 800 \times 10^{-50}$ cm^4 s per photon) should have ample reducing power to transfer an electron to the S–C σ* orbital of a dimethylaryl sulfonium cation, which would cleave the S–C bond and generate acid. We note that triarylamine dialkylsulfonium salts are photosensitive in the near-UV spectrum and generate protons with a photochemical quantum efficiency of $\phi_H{}^+ \approx 0.50$ (*18*).

We also targeted sulfonium groups covalently linked to *bis*(styryl)benzene dyes as two-photon PAGs because (i) covalent attachment of the TPA donor and the sulfonium acceptor helps to ensure rapid forward electron transfer; (ii) triarylamine radical cations are known to be very stable and therefore should facilitate efficient bond cleavage (*18*); (iii) protonated triarylamino groups are strong acids (Ph_3N^+H, $pK_a = -5$) (*19*), so the amine functionality should not inhibit reactions such as the ring-opening polymerization of epoxides; and (iv) non-nucleophilic anions such as PF_6^-, AsF_6^-, or SbF_6^- can be incorporated into these systems.

The compound BSB-S_2 (Fig. 1) was synthesized as shown in fig. S1 and was characterized by spectroscopic and analytical methods (*20*). Solutions of BSB-S_2 in acetonitrile become acidic after irradiation into the lowest energy absorption band [wavelength of maximum absorption (λ_{max}) = 392 nm, extinction coefficient at λ_{max} (ε_{392}) = 5.5×10^4 M^{-1} cm^{-1}]. The quantum efficiency for proton generation was determined to be $\phi_H{}^+ = 0.50 \pm 0.05$ (*21*). This value is comparable to or greater than that of most commercial UV-sensitive PAGs (*22*). It is also consistent with the excited state of the *bis*[(diarylamino)styryl] benzene core being quenched efficiently by transfer of an electron to the dimethylsulfonium group, as evidenced by the low fluorescence quantum efficiency, $\phi_f = 0.013 \pm 0.001$. The acid photogenerated by BSB-S_2 efficiently initiates the polymerization of epoxides (*23*).

The two-photon excitation (TPE) spectrum of Fig. 2A shows that BSB-S_2 exhibits strong TPA from 705 to 850 nm ($\delta > 100 \times 10^{-50}$ cm^4 s per photon) that appears to peak near 710 nm ($\delta = 690 \times 10^{-50}$ cm^4 s per photon) and is consistent with measurements obtained for similar *bis*[(diarylamino)styryl] benzenes (*10*). The TPE and acid yield efficiency spectra (Fig. 2A) exhibit similar features and the acid yield at 745 nm increases quadratically with excitation power (Fig. 2B), as expected for a photochemical process activated by TPA.

There are few reports of two-photon–initiated cationic polymerization of epoxides (*8*, *24*), and each of these involves the use of UV-sensitive PAGs that have very low two-photon sensitivity. We compared the epoxide polymerization sensitivity of BSB-S_2 under near-infrared excitation with four widely used PAGs (Fig. 1): CD1012, CD1012/ITX (1:1.6 molar ratio), TPS, and DPI-DMAS (*20*). The two-photon sensitivity of BSB-S_2 is nearly one order of magnitude greater than that of the best-performing conventional initiator, CD1012/ITX, and more than two orders of magnitude greater than that of TPS, a commercial initiator commonly used in industry. Indeed, we found that BSB-S_2 is a high-sensitivity initiator for cationic polymerization of various epoxide monomers under diverse two-photon excitation conditions utilizing nanosecond or femtosecond pulses (*25*). It is also possible to fabricate freestanding microstructures using solid resin films of BSB-S_2 in the cross-linkable epoxide Epon SU-8 (*26*).

The epoxide-based resins are "negative-tone" systems, in which the exposed regions of the resin become insoluble in a post-exposure development solvent. The polymer structure is then a replica of the exposure pattern. In contrast, positive-tone resists are solid-state systems for which the exposed regions become soluble in a developer. The final structure is then the complement of the exposure pattern. The use of a positive-tone resist in 3D microfabrication is desirable for a number of applications. For example, it should be simpler and more efficient to construct microfluidic devices by excavating a positive-tone material, rather than building up the walls of each microchannel in the structure using a negative-tone resist. In addition, positive-tone resists should help minimize the shrinkage and distortion typically encountered in the photoprocessing of acrylates and other negative-tone resists.

Accordingly, we have developed a solid-state, acid-sensitive, positive-tone, chemically amplified resist, designed for 3D microfabrication by two-photon laser excitation using BSB-S_2 as the PAG. The resist (Fig. 3) is a random copolymer of tetrahydropyranyl methacrylate (THPMA) and methyl methacrylate (MMA). In the presence of acid, an ester cleavage reaction converts the THP-ester groups to carboxylic acid groups and renders the exposed material soluble in aque-

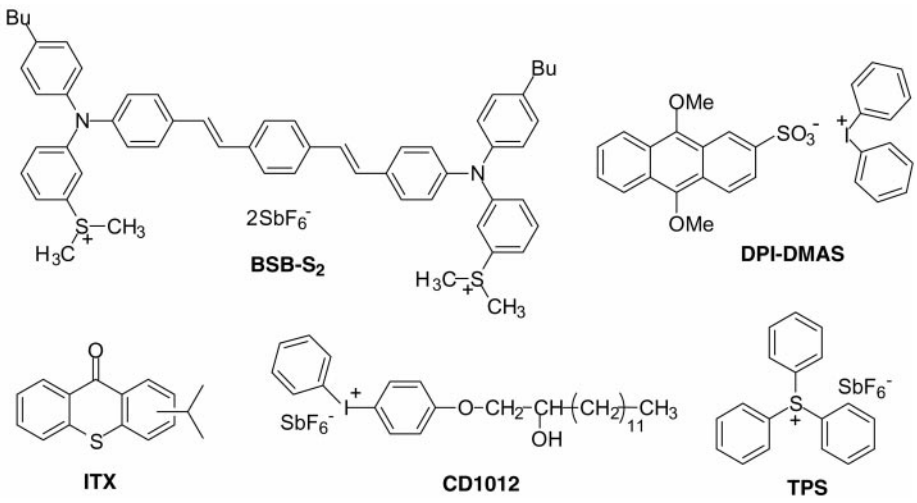

Fig. 1. Structures of BSB-S_2 and the commercially available PAGs used in this study: DPI-DMAS, diphenyliodonium 9,10-dimethoxyanthracenesulfonate; ITX, isopropylthioxanthone; CD1012, [4-[(2-hydroxytetradecyl)oxy]phenyl]phenyliodonium hexafluoroantimonate (Sartomer); and TPS, triphenylsulfonium hexafluoroantimonate.

[1]Department of Chemistry, [2]Optical Sciences Center, University of Arizona, Tucson, AZ 85721, USA. [3]Department of Materials Science and Engineering, Cornell University, Ithaca, NY 14853, USA.

*To whom correspondence should be addressed. E-mail: cober@ccmr.cornell.edu (C.K.O.); jwperry@u.arizona.edu (J.W.P.); smarder@u.arizona.edu (S.R.M.).

ous base developer. The MMA groups provide strength and optical clarity. The carboxylic acid groups generated after exposure and development provide a chemically active site for surface functionalization. This feature is especially useful for the fabrication of microstructures for microfluidic and bioanalytical applications.

To illustrate the use of BSB-S_2 and THPMA-MMA for positive-tone microfabrication, we produced the microchannel structure shown in Fig. 3 using a one-step exposure. The scanning electron micrograph (Fig. 3B) shows that the openings of the channels lie below the film surface and are open to the larger rectangular cavities that extend to the film surface at either end. The two-photon fluorescence images (Fig. 3, C through F), taken after removing the exposed material, reveal that the channels are open and make a continuous connection between the cavities. We have also shown that these channels can be back-filled with liquids, including liquid crystals. This demonstration illustrates that

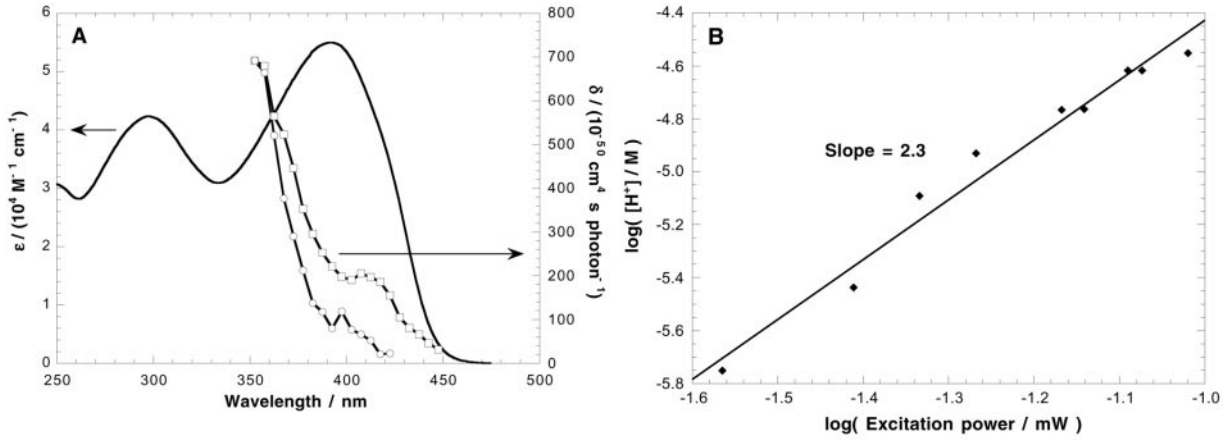

Fig. 2. (**A**) One-photon absorption (solid line), TPE (□), and relative two-photon acid yield efficiency (○) spectra of BSB-S_2 in acetonitrile. The TPE and acid yield spectra are plotted versus half of the excitation wavelength. The one-photon absorption spectrum was recorded using a 2.2×10^{-5} M solution. For the TPE and acid yield spectra, 4.0×10^{-4} M solutions were irradiated in 1-cm path-length fluorescence cells using focused (f = 75 mm) 80-fs pulses from a CW mode-locked Ti:sapphire laser (82 MHz, 8.5-mm-diameter spot size at lens). The TPE spectrum was recorded using the two-photon fluorescence method (*9*, *29*), with fluorescein in water (1.54×10^{-5} M, pH = 11) as a reference. The up-converted fluorescence was detected at 520 nm, and its intensity was proportional to the square of the excitation power, as expected for TPA. The concentration of the photogenerated acid, $[H^+]$, was determined spectrophotometrically after a 30-min exposure. The relative acid yield efficiency at each wavelength was calculated by dividing $[H^+]$ by the ratio of the emission counts and the TPE action cross section of the fluorescein reference $(\langle F(t)\rangle/\phi_f\delta)_{ref}$ (to account for the temporal and spatial dependence of the excitation intensity as a function of wavelength) (*29*) and normalizing to δ of BSB-S_2 at 705 nm. For both experiments, the concentration of BSB-S_2 decreased by less than 2.5% after exposure. (**B**) Plot of log$[H^+]$ against log[excitation power] at 745 nm. The smooth curve is the best fit of a line to the data and has a slope of 2.3, which indicates that the acid yield increases quadratically with the excitation intensity.

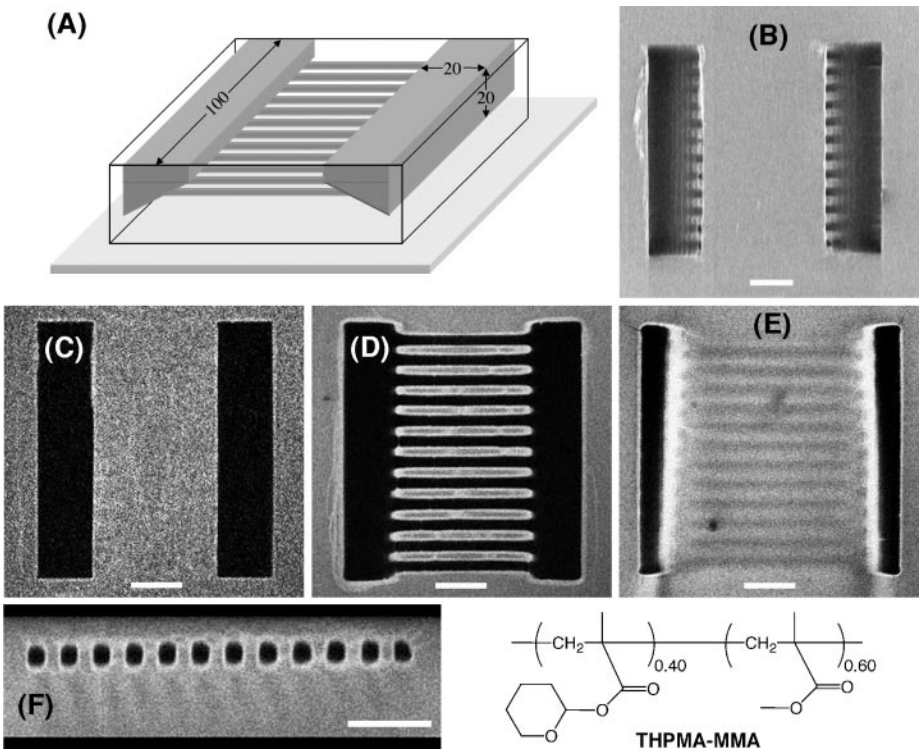

Fig. 3. A 3D microchannel structure fabricated by two-photon exposure of BSB-S_2 in THPMA-MMA. A 50-μm-thick film of 4 wt % BSB-S_2 in THPMA-MMA was exposed in the pattern of the target structure at 745 nm with tightly focused (1.4 N.A.) 80-fs pulses from a Ti:sapphire laser (82-MHz repetition rate) at an average power of 40 μW and a linear scan speed of 50 μm/s. After irradiation, the film was baked for 1 min at 90°C. The target structure was then obtained by dissolving the exposed resin in aqueous 0.26 M tetramethylammonium hydroxide. (**A**) Target structure consisting of two rectangular cavities (width, 100 μm; length, 20 μm; depth, 20 μm) with a sloped side wall that are connected by 12 channels (length, 50 μm; cross section, 4 μm by 4 μm) lying 10 μm below the surface and spaced apart by 8 μm (center to center). (**B**) Scanning electron micrograph of the final structure, viewed normal to the substrate. (**C** to **E**) Two-photon fluorescence images of the final structure (viewed normal to the substrate) (C) at the surface of the film, (D) 10 μm below the surface, and (E) 19 μm below the surface. (**F**) Two-photon fluorescence cross-sectional image of the buried channels. The scale bar in (B) through (F) corresponds to 20 μm.

the BSB-S_2/THPMA-MMA material system can be used to pattern complex 3D structures and suggests that microfluidic structures and even microoptical structures, such as gratings, waveguides, and photonic lattices, can be fabricated readily. The low irradiation power used to pattern the structure also demonstrates the high two-photon sensitivity of this microfabrication material system.

References and Notes

1. S. Maruo, O. Nakamura, S. Kawata, *Opt. Lett.* **22**, 132 (1997).
2. B. H. Cumpston *et al.*, *Nature* **398**, 51 (1999).
3. S. Kawata, H.-B. Sun, T. Tanaka, K. Takada, *Nature* **412**, 697 (2001).
4. S. Maruo, K. Ikuta, *Proc. Soc. Photo-Opt. Instrum. Eng.* **3937**, 106 (2000).
5. H. E. Pudavar, M. P. Joshi, P. N. Prasad, B. A. Reinhardt, *Appl. Phys. Lett.* **74**, 1338 (1999).
6. W. Denk, *Proc. Natl. Acad. Sci. U.S.A.* **91**, 6629 (1994).
7. R. M. Williams, D. W. Piston, W. W. Webb, *Fed. Am. Soc. Exp. Biol. J.* **8**, 804 (1994).
8. K. D. Belfield *et al.*, *J. Phys. Org. Chem.* **13**, 837 (2000).
9. M. Albota *et al.*, *Science* **281**, 1653 (1998).
10. M. Rumi *et al.*, *J. Am. Chem. Soc.* **122**, 9500 (2000).
11. C. G. Willson, H. Ito, J. M. J. Fréchet, T. G. Tessier, F. M. Houlihan, *J. Electrochem. Soc.* **133**, 181 (1986).
12. J. M. J. Fréchet *et al.*, *J. Imag. Sci.* **30**, 59 (1986).
13. J. M. J. Fréchet *et al.*, in *Functional Polymers*, D. E. Bergbreiter, C. R. Martin, Eds. (Plenum, New York, 1989), pp. 193–200.
14. R. W. Angelo *et al.*, U.S. Patent 5,047,568 (1991).
15. R. W. Angelo *et al.*, U.S. Patent 5,102,772 (1992).
16. F. D. Saeva, *Adv. Electr. Trans. Chem.* **4**, 1 (1994).
17. F. D. Saeva, D. T. Breslin, P. A. Martic, *J. Am. Chem. Soc.* **111**, 1328 (1989).
18. W. Zhou, S. M. Kuebler, D. Carrig, J. W. Perry, S. R. Marder, *J. Am. Chem. Soc.* **124**, 1897 (2002).
19. J. March, *Advanced Organic Chemistry* (Wiley, New York, ed. 3, 1985).
20. Details of the molecular synthesis and polymerization studies are available on *Science* Online at www.sciencemag.org/cgi/content/full/296/5570/1106/DC1.
21. Solutions of BSB-S_2 in acetonitrile (4.0×10^{-4} M) were irradiated at 400 nm with either a Xenon lamp or a frequency-doubled mode-locked Ti:sapphire laser. At this concentration, more than 99% of the light was absorbed. The photogenerated acid was titrated by the addition of excess rhodamine B base in acetonitrile (6.0×10^{-5} M after addition) and quantified spectrophotometrically from the absorbance of protonated rhodamine B base (*27*). The acid yield increased linearly with both the excitation intensity and time, consistent with acid generation being initiated by one-photon excitation.
22. M. Shirai, M. Tsunooka, *Prog. Polym. Sci.* **21**, 1 (1996).
23. Irradiating 4 ml of BSB-S_2 at 8×10^{-7} M in 80% (by volume) cyclohexene oxide in dichloromethane at 419 nm yielded polymer that precipitated after the addition of methanol.
24. Y. Boiko, J. M. Costa, M. Wang, S. Esener, *Opt. Express* **8**, 571 (2001).
25. Freestanding columns of cross-linked polymer were generated when a 10 mM solution of BSB-S_2 in 20% Epon SU-8 (Shell)/80% 4-vinyl-cyclohexene dioxide by weight was irradiated at 745 nm for 5 s at a threshold pulse energy of 940 μJ, using focused 5-ns pulses (at a 10-Hz repetition rate, 500-mm focal length, and 5-mm-diameter spot size at the focusing lens). Under similar conditions, BSB-S_2 also initiates the polymerization of 20% SU-8/80% cyclohexene oxide, neat Araldite CY179MA, and solid films of SU-8.
26. Freestanding microstructures were fabricated (*2*, *28*) by irradiating solid thin films of 1 weight % (wt %) BSB-S_2 in SU-8 using tightly focused [numerical aperture (NA) = 1.4] 80-fs pulses (at an 82-MHz repetition rate, 745 nm) at average powers as low as 2.4 mW and then dissolving the unexposed resin in an organic solvent.
27. G. Pohlers, J. C. Scaiano, R. Sinta, *Chem. Mater.* **9**, 3222 (1997).
28. S. M. Kuebler *et al.*, *J. Photopolym. Sci. Technol.* **14**, 657 (2001).
29. C. Xu, W. W. Webb, *J. Opt. Soc. Am. B* **13**, 481 (1996).

30. Support from the Air Force Office of Scientific Research (grants F49620-99-1-0019 and F49620-97-1-0014), NSF (grants CHE-0107105 and DMR-9975961), the Office of Naval Research (grants N00014-95-1319 and N000141-01-1-0633), the NSF-funded Cornell Nanobiotechnology Center, and the Defense University Research Instrumentation Program (grants N00014-99-1-0541 and F49620-00-1-0161) is gratefully acknowledged.

30 November 2001; accepted 19 March 2002

A Possible Tektite Strewn Field in the Argentinian Pampa

P. A. Bland,[1]* C. R. de Souza Filho,[2] A. J. T. Jull,[3] S. P. Kelley,[4] R. M. Hough,[5] N. A. Artemieva,[6] E. Pierazzo,[7] J. Coniglio,[8] L. Pinotti,[8] V. Evers,[9] A. T. Kearsley[10]

Impact glass associated with 11 elongate depressions in the Pampean Plain of Argentina, north of the city of Río Cuarto, was suggested to be proximal ejecta related to a highly oblique impact event. We have identified about 400 additional elongate features in the area that indicate an aeolian, rather than an impact, origin. We have also dated fragments of glass found at the Río Cuarto depressions; the age is similar to that of glass recovered 800 kilometers to the southeast. This material may be tektite glass from an impact event around 0.48 million years ago, representing a new tektite strewn field.

Comets and asteroids that impact planets create circular craters at impact angles between ~15° and 90° (measured from the surface); when the angle θ is less than ~15°, craters become elongate in shape. On Earth, the only confirmed low-angle impact structures are the series of elongate craters at Río Cuarto, Argentina, estimated to be <0.01 million years (Ma) (*1*) to <0.005 Ma (*2*, *3*) in age. Río Cuarto is also the largest object known to have impacted Earth in the last 0.1 Ma, an impact that may have been witnessed by early inhabitants of the Pampean Plain (*1*). The largest feature (64°10′W, 32°45′S) has dimensions of 4.5 km by 1.1 km and is considered to correspond to the first impact; an impactor initially 150 to 300 m in diameter then fragmented and ricocheted to the south to produce 10 additional elongate depressions (*1*). Impact formation of the depressions was questioned (*4*), but samples of meteorite, and detailed analysis of glass fragments found at the site, supported the impact hypothesis (*1*, *5*).

Río Cuarto glass is typically vesicular, with abundant loess inclusions, and lower surfaces that appear to be sand casts (*1*, *5*). Vesicle-poor splash forms (elongate drops) are also common (*1*, *5*). Although most samples do not show evidence of much meteoritic contamination, some fragments exhibit high Cr [>1000 parts per million (ppm)] and Ni (1 to 2 weight %) concentrations, and one has metallic Fe and Fe-Ni spherules (*5*). Siderophile-element abundance and rare earth element pattern suggest a chondritic impactor (*6*). In addition, very low water content (characteristic of tektites and other impact glasses) is typical; vesicular glass contains ~0.1 weight % water, whereas splash-form glass contains 0.06 weight % (*5*). The presence of lechatelierite (*5*), homogeneous oxide distribution, and high silica content are additional characteristics in common with tektites (*1*). Overall, the glass has a composition similar to that of the loessoid sediments that cover the Pampa (*1*, *7*). Because loess only occurs to a depth of <50 m over a metamorphic basement, it was suggested that the glass originated in a low-angle impact that did not excavate deeply (*5*).

We have conducted an extensive remote-sensing study of the Río Cuarto site and the surrounding Pampean Plain, using CORONA and EOS Terra-ASTER multispectral, high-resolution satellite imagery. This survey reveals several hundred elongate depressions with high length-to-width ratios (Figs. 1, S1, and 2); 403 are >200 m in their long axes, 201 >1 km, and 6 >5 km. Long-axis orientations vary throughout the region: north-

[1]Planetary and Space Sciences Research Institute, The Open University, Milton Keynes MK7 6AA, UK. [2]Instituto de Geociências, Universidade Estadual de Campinas, Campinas, Brazil. [3]NSF–Arizona Accelerator Mass Spectrometry Laboratory, University of Arizona, 1118 East Fourth Street, Tucson, AZ 85721, USA. [4]Department of Earth Sciences, The Open University, Milton Keynes MK7 6AA, UK. [5]Earth and Planetary Sciences, Western Australian Museum, Francis Street, Perth, Western Australia 6000. [6]Institute for Dynamics of Geospheres, Russian Academy of Sciences, Leninsky Prospect 38/6, Moscow, Russia 117939. [7]Planetary Science Institute, Tucson, AZ 85705, USA. [8]Departamento de Geología, Universidad Nacional de Río Cuarto, 5800 Río Cuarto, Córdoba, Argentina. [9]Institute of Educational Technology, The Open University, Milton Keynes MK7 6AA, UK. [10]Geology (Biological and Molecular Sciences), Oxford Brookes University, Headington, Oxford OX3 OBP, UK.

*To whom correspondence should be addressed. E-mail: p.a.bland@open.ac.uk